Journal of Radioanalytical and Nuclear Chemistry (2020) 323:885–895
https://doi.org/10.1007/s10967-019-07001-x

Measurement of natural radioactivity concentrations and chemical composition of coal and its post-combustion residues in KSA

Dalal A. Aloraini[1] · Khaled M. El-Azony[2]

Received: 25 September 2019 / Published online: 3 January 2020
© Akadémiai Kiadó, Budapest, Hungary 2020

Abstract

The variable values of ^{226}Ra, ^{228}Ra and ^{40}K were identified in coal and coal combustion residuals (CCR) samples to redistribute radionuclides using ^{228}Ra/^{226}Ra activity ratios in CCRs and compared to their values in the corresponding feed coal. NORM concentrations in CCRs were found to be 6–12 times higher than the original coal. The effective dose rates in the original coal were calculated and ranged from 14.9 ± 0.9 to 370.3 ± 22.2 μSv year^{-1}, whereas in CCRs ranged from 257.5 ± 20.6 to 1797.5 ± 143.8 μSv year^{-1}. The average concentration of ^{40}K (120 Bq kg^{-1} per 1% K_2O in CCRs) was calculated. The chemical composition indicates that the majority of CCR samples are Type C, which has a high calcium oxide ratio, high melting points and low deposition.

Keywords Coal combustion residues · CCRs · Naturally occurring radioactive materials · NORM · Chemical composition

Introduction

Despite the increased thermal power from coal combustion, however, residues often contain high radioactive concentrations as natural occurring radioactive materials (NORM) and are used in the manufacture of certain building materials such as cement, concrete and bricks [1]. Since the 1960s, coal and CCR radioactivities have been identified [2, 3], due to the longevity of the common NORM (^{238}U, ^{226}Ra, ^{210}Pb, ^{232}Th, ^{228}Ra, and ^{40}K) [4–6]. Coal is categorized according to the concentrations of NORM, either high concentrations of NORM at low concentrations of sub-bituminous, brown and lignite, or low concentrations of NORM at high concentrations of bituminous [7, 8].

Some hazardous trace elements such as cadmium (Cd), arsenic (As), molybdenum (Mo), vanadium (V), mercury (Hg) and various acid gasses are detected during coal burning [9]. Several countries used the CCRs to manufacture Portland cement [10] and concrete [11] as allowed by the European Standard EN 197-1. There are 27 different common products of cement classified into five categories. Composite cement is the fifth category containing 18–50% of coal fly ash. A reference level (1 mSv year^{-1}) [12] has been determined for external indoor exposure owing to gamma radiation emitted by building materials [13]. Many industrial residues are presently being studied as prospective construction materials [14].

On the other hand, European waste has studied and identified the chemical composition of coal [15, 16] and CCRs as non-hazardous waste [17, 18]. Coal contains predominantly carbon with variable quantities of other elements; primarily hydrogen, oxygen, sulfur and nitrogen [16]. The chemical composition of coal has been converted into CO_2 and CH_4 by breaking chemical bonds from hemicellulose, cellulose and most biomass and has lost up to 70% of the weight at 550 °C. Unburnt alkaline sulfate particles are formed at an elevated temperature and gain comparative weight. The elements of low melting point may agglomerate to form clusters of particles of high melting point [16]. Most of the carbon was eliminated at temperatures above 550 °C, increasing the proportions of elements with high melting points. Carbon

Electronic supplementary material The online version of this article (https://doi.org/10.1007/s10967-019-07001-x) contains supplementary material, which is available to authorized users.

✉ Khaled M. El-Azony
azonychemist@gmail.com

[1] Physics Department, College of Science, Princess Nourah Bint Abdulrahman University, Riyadh, Kingdom of Saudi Arabia

[2] Radioactive Isotopes and Generators Department, Hot Labs. Center, Atomic Energy Authority, P. O. Box 13759, Cairo, Egypt

values usually ranged 15–25%, whereas oxygen remains in the form of oxides, and slightly increased carbonates and sulfates [16]. The high peaks of silicon in coal (40%) compared to other elements. Ironically, K and Ca are the main elements contained in the slag as well as the first components of most coal samples exceeding 15%, while Mg values are nearly constant 3–5% values.

Electricity production in Kingdom of Saudi Arabia (KSA) depends on the main sources of energy are natural gas and petroleum. Domestic power generation demand is set to increase and looks forward to supplying it from the coal and renewable energy. Some countries of the Gulf Cooperation Council (GCC) used coal for coal-fired plants, but not so far in KSA. Several factors point to the possibility of using coal as a prospective source of electricity and cement production in KSA, such as lower operating costs and higher global reserves (990 billion tons of current consumption, sufficient for 150 years) [19]. Coal is expected to quickly play an important role in the electricity and cement sector in Saudi Arabia. Coal is currently used for narghile (hookah, shisha, goza) and grill of different types of meat, many Arab countries use coal as fuel for smoking tobacco. The present study is therefore a pre-emptive step for KSA to select high-quality coal by measuring NORM and chemical compositions of various kinds of coal on the local market and calculating adsorbed dose (nGy h^{-1}) and effective dose (mSv $year^{-1}$) before and after coal combustion.

Experimental

Samples preparation

Twenty-seven coal samples were purchased from the local market of the Kingdom of Saudi Arabia, and prepared for gamma analysis and elemental analysis. Eighteen samples were burned in order to analyze the CCRs (slag by-products and remaining solids). The samples were homogenized and packed with standard size cups (75 ml) and tightly sealed, then stored for more than a month to reach secular equilibrium of ^{226}Ra and to prevent radon gas escape. In order to determine efficiency calibration, reference material (RGU-1) was also packed into the same standard size cups. Gamma-analysis was used to measure the samples and reference material.

Analytical techniques

Gamma-spectrometry analysis

A coaxial P-type (relative efficiency 50%) high purity germanium detector (HPGe) was used. A low level background due to the existence of a lead shield to protect the detector. The RGU-1 was used as a reference material for the HPGe detector efficiency calibration. It was verified that radium-226 is in equilibrium with uranium content. The certified activity of uranium is 400 ppm, which refers to 4960 Bq kg^{-1}. To create the efficiency calibration curve, the ^{226}Ra daughters (^{214}Pb and ^{214}Bi) were used. A polynomial fitting of the fourth degree was performed to obtain the best R^2 value (≈ 0.997).

Radioisotopes ^{226}Ra and ^{228}Ra explained that concentrations of radioactivity ranged from below the detection limit to 13.8 and 17 Bq kg^{-1}, respectively, while ^{40}K ranged from 40.0 to 553 Bq kg^{-1} (53.0% potassium content).

Radium-226 was measured by achieving secular equilibrium with its daughter ^{214}Pb ($t_{1/2} = 26.9$ min) at 295.2 keV ($I_\gamma = 19.3\%$), 351.93 keV ($I_\gamma = 37.6\%$), and ^{214}Bi ($t_{1/2} = 19.7$ min) at 609.31 keV ($I_\gamma = 46.1\%$), 1120.29 keV ($I_\gamma = 15.1\%$), 1764.49 keV ($I_\gamma = 15.4\%$). Radium-228 was determined at 911.2 keV ($I_\gamma = 25.8\%$) by measuring the ^{228}Ac ($t_{1/2} = 6.15$ h).

Potassium-40 was estimated at $E_\gamma = 1490.83$ keV, $I_\gamma = 11\%$. The efficiency of each transition line was either determined by direct comparison of the energy lines in the reference material or obtained from the above-mentioned efficiency calibration curve.

The reference sample and the measured samples subtracted the background of each energy line. The detection limit based on the Currie detection limit method was calculated as follows:

$$\text{MDA (counts)} = 2.7 + 4.65 \times \sqrt{\text{BG}}$$

The detection limit for each radionuclide was calculated individually. The calibration was tested against IAEA proficiency and no more than 5% bias was found.

XRF analysis

The JSX-3222 analyzer, Japan (type JEOL) is an energy-dispersive X-ray fluorescent spectrometer used to evaluate the constituent elements of coal consumed by KSA. Samples were assessed using loose powders were prepared for XRF that is one of the most important, steps in achieving accuracy. The range of elements measured ranges from sodium (Na) to uranium (U).

Results and discussion

Radioactive analysis

The classification of coal consumed in Saudi Arabia based on radioactivity concentrations is shown in Table 1. The ^{226}Ra and ^{228}Ra were indirectly determined by measuring

Table 1 Activity concentrations of ^{226}Ra, ^{228}Ra and ^{40}K in the coal (BC) and CCRs (AC) (Bq kg^{-1}) dry weight

Sample ID	Country of Origin	Trade name of coal	^{226}Ra (Bq kg^{-1}) ± 1σ		^{228}Ra (Bq kg^{-1}) ± 1 σ		^{40}K (Bq kg^{-1}) ± 1 σ		^{226}Ra + ^{228}Ra	^{226}Ra + ^{228}Ra	(Total Ra)$_{AC}$/(Total Ra)$_{BC}$	Mean
			BC	AC	BC	AC	BC	AC	BC	AC		
1	Malaysia	Middle East Charcoa	4 ± 0.6		LLD		82.6 ± 5					11.51
2		Ghazal BBQ	6.8 ± 1	77.8 ± 3.9	7 ± 1.5	81 ± 4.1	174 ± 34	1130 ± 56	13.8 ± 2.5	158.8 ± 8.0	11.51	
3	Thailand	Shishaco	2 ± 0.5		LLD		81.6 ± 5					10.10
4		Rehlat Saied	6.5 ± 0.3	64.6 ± 3.2	9.3 ± 2	95 ± 4.2	51.1 ± 4	435 ± 22	15.8 ± 2.3	159.6 ± 7.4	10.10	
5	UEA	Fire top	3.8 ± 0.3	37.1 ± 1.1	5 ± 0.9	49.1 ± 2.5	300.4 ± 5	1958 ± 38	8.8 ± 1.2	86.2 ± 3.6	9.80	9.80
6	Spain	Orinex	8 ± 1.3	56 ± 2.2	7 ± 1.5	50.3 ± 2.5	251 ± 14	1288 ± 64	15 ± 2.8	106.3 ± 4.7	7.09	7.09
7	USA	King Sford	5.7 ± 1	50.3 ± 2.6	3 ± 0.4	27.8 ± 2	347.8 ± 3	1900 ± 15	8.7 ± 1.4	78.1 ± 4.6	8.98	8.98
8	China	Barbecue charcoal	11.1 ± 1.7	65.9 ± 2.2	19.2 ± 3.5	122 ± 6.1	553 ± 30	2150 ± 108	30.3 ± 5.2	187.9 ± 8.3	6.20	6.08
9		Toppy	2.9 ± 0.5	15.5 ± 0.8	1.3 ± 0.2	9 ± 0.7	51.9 ± 3	207 ± 10.4	4.2 ± 0.7	24.5 ± 1.5	5.83	
10		Super Kima	13.8 ± 2.2	51.7 ± 2.6	17 ± 3	71.6 ± 3.6	268 ± 15	1050 ± 52.5	30.8 ± 5.2	123.3 ± 6.2	4.00	
11		Burnable charcoal	3.5 ± 0.6	28.5 ± 1.0	4 ± 1	33.5 ± 1.7	168 ± 9	320 ± 66	7.5 ± 1.6	62 ± 2.7	8.27	
12	Indonesia	Volcano	LLD		LLD		68 ± 4					6.20
13		Earthquake	2.2 ± 0.5	24 ± 1.3	2 ± 0.5	23.7 ± 1.2	109 ± 6	1337 ± 16.9	4.2 ± 1.0	47.7 ± 2.5	11.36	
14		Mowfoor	4.2 ± 0.6	20 ± 1.4	5 ± 0.5	26.8 ± 1.3	99 ± 6	716 ± 35.8	9.2 ± 1.1	46.8 ± 2.7	5.09	
15		Royal BBQ	LLD		LLD		38 ± 3					
16		Al Nakhla coal	LLD		LLD		40 ± 3.5					
17		Copra	LLD		LLD		103 ± 6					
18		Cococha	LLD	12.1 ± 0.5	7.3 ± 1.5	14.3 ± 1	58.4 ± 3.1	321 ± 16.1	7.3 ± 1.5	26.4 ± 1.5	3.62	
19		Tropicana	LLD	14.9 ± 0.5	6.9 ± 1.4	18.2 ± 1	139 ± 7.5	599 ± 30	6.9 ± 1.4	33.1 ± 1.5	4.80	
20	Somalia	Somali Charcoal	LLD		LLD		71 ± 5					
21	South Africa	Southafrica coal	LLD		LLD		66 ± 4					
22	Paraguay	Samba	LLD		11 ± 2.3		66.8 ± 4.1					
23	KSA	Charcoal	LLD	13 ± 1.3	6 ± 1.3	21.6 ± 1	100.6 ± 5.5	913 ± 5.7	6 ± 1.3	34.6 ± 2.3	5.77	7.60
24		Al-Hijaz	LLD	25.1 ± 1.7	7.3 ± 1.5	44.5 ± 2.2	99 ± 5.4	1990 ± 59.5	7.3 ± 1.5	69.6 ± 3.9	9.53	
25		Medina	LLD	10 ± 0.5	8.5 ± 1.8	56.6 ± 0.8	76.7 ± 4.1	277 ± 13.9	8.5 ± 1.8	66.6 ± 1.3	7.84	
26		Gwyn	LLD	7.2 ± 0.4	LLD	15.4 ± 0.8	49 ± 3	462 ± 23.1				
27		Bamboo charcoal	8.5 ± 1	59.6 ± 2.2	10 ± 2.1	71.5 ± 3.6	238 ± 13	1330 ± 66.5	18.5 ± 3.1	131.1 ± 5.8	7.09	

^{214}Bi and ^{214}Pb as daughters of ^{226}Ra, ^{228}Ac and ^{212}Pb as daughters of ^{228}Ra [20]. Table 1 shows total radioactivity of Ra_{AC} in CCRs 6–12 times higher than the total radioactivity of Ra_{BC} in feed coal, which may be attributed to the removal of approximately 10–15% of carbon during the coal burning [21]. The average values of the ^{226}Ra, ^{228}Ra and ^{40}K before the burning of the coal are 6, 11 and 138 Bq kg^{-1}, respectively, whereas the post-burning values are 30, 50 and 777 Bq kg^{-1}. By comparing our data with the literature before coal burning, the average values of ^{226}Ra are found to be relatively lower than the literature values (16.2 Bq kg^{-1}) [9], but agree with the literature values of ^{228}Ra and ^{40}K (13.1 and 133.7 Bq kg^{-1}, respectively) [9]. After the coal burning, the average value of ^{226}Ra in our data is still lower than the literature value (55 Bq kg^{-1}), our data are consistent with the literature data for ^{228}Ra (50 Bq kg^{-1}) and higher than the value of ^{40}K (433 Bq kg^{-1}) [9]. The low concentration of ^{226}Ra may be due to uranium-238 (^{226}Ra parent) found mainly in sedimentary rock organic layer materials, which can be easily removed during the combustion process, while ^{232}Th (^{228}Ra parent) occurs in inorganic layers [22]. On the other hand, burning organic matter leads to an increase in natural radionuclide concentrations in CCRs depending on the physical and chemical composition of coal as well as the circumstances of the combustion process and can be attributed to radionuclide accumulation in the form of oxides in CCRs [22].

Redistribution of radionuclides in coal and CCRs was investigated by calculating the proportions of ^{228}Ra/^{226}Ra, which are relatively higher in CCRs than the feed coal as shown in Table 2. The ^{228}Ra/^{226}Ra ratios in CCRs and feed coal are consistent with the ratios reported in literature [6, 21, 23]. The ^{238}U and ^{232}Th are found in radioactive equilibrium (secular equilibrium) with their decay products (their daughters) and expressed as the ratios ^{238}U/^{226}Ra and ^{232}Th/^{228}Ra equivalent to the unit in the closed system [21, 24]. The average ratio of ^{228}Ra/^{226}Ra in soil is supposed to be about 1.2 equal to the average Th/U activity ratio in continental crust. In CCRs, the average total radium radioactivity was estimated and found to be about 100 Bq kg^{-1}, which is 1.5 times higher than in the soil (about 70 Bq kg^{-1}). Most coal samples have a ratio of ^{228}Ra/^{226}Ra greater than one, meaning that the concentration of ^{226}Ra is lower than concentration of ^{228}Ra except for some samples such as Orinex, King Sford, Toppy and Earthquake. The ^{228}Ra/^{226}Ra ratios in CCR samples were slightly increased relative to their values in the feed coal indicating that the ^{226}Ra removal due to the combustion process is lower than ^{228}Ra.

Absorbed dose

According to the European Radiation Protection Guide 122 [25], for the materials to be used to make any use limitation decision, a dose assessment of the situation should be carried out [25]. A scenario for calculating the effective annual dose of coal radioactivity using the Markkanen model was proposed [26]. The conversion factor used to calculate the absorbed gamma dose rate D (nGy h^{-1}) for ^{226}Ra, ^{232}Th and ^{40}K corresponds to 0.92, 1.1 and 0.08 nGy h^{-1} per Bq kg^{-1}, respectively [25–27] as in Eq. (1)

$$D\ (\text{nGy h}^{-1}) = 0.087A_{\text{K}} + 0.92A_{\text{Ra}} + 1.1A_{\text{Th}} \quad (1)$$

Table 3 indicates the absorbed dose rates in feed coal and CCRs range from 3 ± 0.2 to 75.6 ± 3.8 and from 40.7 ± 2.9 to 366.8 ± 25.7 nGy h^{-1} with the average of 19.5 and 165 nGy h^{-1}, respectively, whereas the average worldwide value (55 nGy h^{-1}) [25, 28]. The conversion coefficient (0.7 Sv Gy^{-1}) was used to calculate the annual effective dose rates as the following equation:

$$\text{Effective dose rate } (\mu\text{Sv year}^{-1}) = D \times 7000(\text{h year}^{-1}) \times 0.7(\text{Sv Gy}^{-1}) \times 10^{-3} \quad (2)$$

The effective dose rates calculated in feed coal ranged from 14.9 ± 0.9 to 370.3 ± 22.2 μSv year^{-1}, while from 257.5 ± 20.6 to 1797.5 ± 143.8 μSv year^{-1} ranged in CCRs that higher than those reported in the literature resulting of terrestrial radionuclides (460 μSv year^{-1}) [29, 30].

Chemical composition

The proportions of the chemical constituents in the feed coal and CCRs were determined using the XRF technique as shown in Table 4. The variable element ratios depend on the physical and chemical properties of coal, which form metal oxides in CCRs after the feed coal burning in oxygen [16]. It is notable that the average concentration of silicon, potassium, calcium and iron in feed coal is 13, 11, 49 and 16%, respectively, as shown in Table 4. The low concentrations of elements Al, Ti, Mn, Zn, Rb, Sr and Zr ranged from less than 1 to 5% in the feed coal. Most CCR samples contain Si, K and Ca with an average concentration of 18, 9% and 49%, respectively. Zn, Rb, and Zr ratios are almost constant at around 1% for most samples, while Ti ratios range from 1 to 3%.

In this study, potassium is the only element could be measured by XRF and gamma analysis before and after the combustion to determine the volatilization ratio and the

Table 2 Average $^{228}Ra/^{226}Ra$ rations in the coal (BC) and CCRs (AC)

Sample ID	Country of origin	Trade name of coal	BC					AC				
			^{226}Ra (Bq kg^{-1})	^{228}Ra (Bq kg^{-1})	$^{228}Ra/^{226}Ra$	Th/U	Referencess	^{226}Ra (Bq kg^{-1})	^{228}Ra (Bq kg^{-1})	$^{228}Ra/^{226}Ra$	Th/U	References
1	Malaysia	Middle East Charcoa	4 ± 0.6	LLD								
2		Ghazal BBQ	6.8 ± 14%	7 ± 21%	1.03 ± 35%		Lauer [21]	77.8 ± 5%	81 ± 5%	1.04 ± 10%		Lauer [21]
3	Thailand	Shishaco	2 ± 25%	LLD								
4		Rehlat Saied	6.5 ± 4.6%	9.3 ± 21.5%	1.43 ± 26%			64.6 ± 5%	95 ± 4%	1.47 ± 9%		
5	UEA	Fire top	3.8 ± 8%	5 ± 18%	1.32 ± 26%			37.1 ± 3%	50.1 ± 5%	1.35 ± 8%		
6	Spain	Orinex	8 ± 16%	7 ± 21%	0.88 ± 37%	0.92	Swanson [23]	56 ± 4%	50.3 ± 5%	0.9 ± 9%	0.92	Swanson [23]
7	USA	King Sford	5.7 ± 18%	3 ± 13%	0.53 ± 31%	0.54	Beck [6]	50.3 ± 5%	27.8 ± 12%	0.55 ± 17%	0.54	Beck [6]
8	China	Barbecue charcoal	11.1 ± 15%	19.2 ± 18%	1.73 ± 33%			65.9 ± 3%	122 ± 5%	1.85 ± 8%		
9		Toppy	2.9 ± 17%	1.3 ± 15%	0.5 ± 33%	0.54	Beck [6]	15.5 ± 5%	9 ± 8%	0.58 ± 13%	0.54	Beck [6]
10		Super Kima	13.8 ± 16%	17 ± 18%	1.23 ± 34%			51.7 ± 5%	71.6 ± 5%	1.38 ± 10%		
11		Burnable charcoal	3.5 ± 17%	4 ± 25%	1.14 ± 42%	1.13	Swanson [23]	28.5 ± 3.5%	33.5 ± 5%	1.18 ± 8.5%	1.13	Swanson [23]
12	Indonesia	Volcano	LLD	LLD								
13		Earthquake	2.2 ± 23%	2 ± 25	0.91 ± 48%	0,92	Swanson [23]	24 ± 5%	23.7 ± 5%	0.99 ± 10%	0.92	Swanson [23]
14		Mowfoor	4.2 ± 14%	5 ± 10%	1.19 ± 24%	1.13	Swanson [23]	20 ± 7%	26.8 ± 5%	1.19 ± 12%	1.13	Swanson [23]
15		Royal BBQ	LLD	LLD								
16		Al Nakhla coal	LLD	LLD								
17		Copra	LLD	LLD								
18		Cococha	LLD	7.3 ± 21%				12.1 ± 4%	14.3 ± 7%	1.18 ± 11%	1.13	Swanson [23]
19		Tropicana	LLD	6.9 ± 20%				14.9 ± 3%	18.2 ± 5.5%	1.22 ± 8.5%	1.13	Swanson [23]
20	Somalia	Somali Charcoal	LLD	LLD								
21	South Africa	Southafrica coal	LLD	LLD								
22	Paraguay	Samba	LLD	11 ± 2.3								
23	KSA	Charcoal	LLD	6 ± 1.3				13 ± 1.3	21.6 ± 1	1.66		
24		Al-Hijaz	LLD	7.3 ± 1.5				25.1 ± 1.7	44.5 ± 2.2	1.77		
25		Medina	LLD	8.5 ± 1.8				10 ± 0.5	56.6 ± 0.8			
26		Gwyn	LLD	LLD				7.2 ± 0.4	15.4 ± 0.8	2.14		
27		Bamboo charcoal	8.5 ± 12%	10 ± 21%	1.18 ± 33%	1.13	Swanson [23]	59.6 ± 2.2	71.5 ± 3.6	1.20	1.13	Swanson [23]

Table 3 Absorbed dose (nGy h^{-1}) and annual effective dose (μSv $year^{-1}$) due to exposure to the coal (BC) and the CCRs (AC)

Sample ID	Country of origin	Trade name of coal	BC		AC	
			Absorbed dose (nGy h^{-1})	Effective dose rate (μSv $year^{-1}$)	Absorbed dose (nGy h^{-1})	Effective dose rate (μSv $year^{-1}$)
1	Malaysia	Middle East Charcoa	10.2 ± 0.5	50.2 ± 3.0		
2		Ghazal BBQ	27.9 ± 1.4	136.6 ± 8.2	251.1 ± 17.6	1722.6 ± 137.8
3	Thailand	Shishaco	8.4 ± 0.4	41.0 ± 2.5		
4		Rehlat Saied	20.3 ± 1.0	99.5 ± 6.0	198.7 ± 13.9	973.6 ± 77.9
5	UEA	Fire top	33.0 ± 1.7	161.8 ± 9.7	244.8 ± 17.1	1199.5 ± 96.0
6	Spain	Orinex	35.1 ± 1.8	172.2 ± 10.3	209.9 ± 14.7	1028.5 ± 82.3
7	USA	King Sford	36.4 ± 1.8	178.2 ± 10.7	228.9 ± 16.0	1121.6 ± 89.7
8	China	Barbecue charcoal	75.6 ± 3.8	370.3 ± 22.2	366.8 ± 25.7	1797.3 ± 143.8
9		Toppy	8.3 ± 0.4	40.4 ± 2.4	40.7 ± 2.9	199.4 ± 16.0
10		Super Kima	52.8 ± 2.6	258.9 ± 15.5	210.3 ± 14.7	1030.5 ± 82.4
11		Burnable charcoal	21.1 ± 1.1	103.2 ± 6.2	88.7 ± 6.2	434.6 ± 34.8
12	Indonesia	Volcano	5.4 ± 0.3	26.7 ± 1.6		
13		Earthquake	12.9 ± 0.7	63.4 ± 3.8	155.1 ± 10.9	760 ± 60.8
14		Mowfoor	17.3 ± 0.9	84.7 ± 5.1	105.2 ± 7.4	515.5 ± 41.2
15		Royal BBQ	3.0 ± 0.2	14.9 ± 0.9		
16		Al Nakhla coal	3.2 ± 0.2	15.7 ± 1.0		
17		Copra	8.2 ± 0.4	40.4 ± 2.4		
18		Cococha	12.7 ± 0.6	62.2 ± 3.7	52.5 ± 3.7	257.3 ± 20.6
19		Tropicana	18.7 ± 0.9	91.7 ± 5.5	81.7 ± 5.7	400.3 ± 32.0
20	Somalia	Somali Charcoal	5.7 ± 0.3	27.8 ± 1.7		
21	South Africa	Southafrica coal	5.3 ± 0.3	25.9 ± 1.6		
22	Paraguay	Samba	17.4 ± 0.9	85.5 ± 5.1		
23	KSA	Charcoal	14.7 ± 0.7	71.8 ± 4.3	108.8 ± 7.6	533.1 ± 42.6
24		Al-Hijaz	16.0 ± 0.8	78.2 ± 4.7	231.2 ± 16.2	1132.9 ± 90.6
25		Medina	15.5 ± 0.8	75.9 ± 4.6	93.6 ± 6.6	458.6 ± 36.7
26		Gwyn	3.9 ± 0.2	19.2 ± 1.2	60.5 ± 4.2	296.5 ± 23.7
27		Bamboo charcoal	37.9 ± 1.9	185.5 ± 11.1	239.9 ± 16.8	1175.5 ± 94.0

enrichment factor (E_f). The potassium enrichment factor was calculated by dividing ^{40}K radioactivity in CCRs on its radioactivity in feed coal as in Eq. (3).

$$E_f = \frac{(A_{40_K})_{CCRs}}{(A_{40_K})_{Coal}} \tag{3}$$

Where, the specific activities of ^{40}K in CCRs and their feed coal represent $(A_{40_K})_{CCRs}$ and $(A_{40_K})_{Coal}$. The majority of coal has a higher potassium volatilization rate than its enrichment, as shown in Fig. 1 as in Bamboo charcoal, where the volatilization rate is 53% compared to the 6% enrichment factor. These results may be due to potassium has a low melting point (63 °C) as an alkali metal, making it more volatile and increasing the rate of its evaporation during the process of combustion. Table 5 indicates that the average concentration of ^{40}K in CCRs was found to be 120 Bq kg^{-1} per 1% K_2O, a half-value (252 Bq kg^{-1}) reported by Mohanty in 2004 [31].

The base/acid ratio ($R_{b/a}$) calculated by Eq. (4) is shown in Table 6 (Electronic Supplementary Material):

$$R_{b/a} = \frac{Fe_2O_3 + K_2O + CaO + MgO}{SiO_2 + TiO_2 + Al_2O_3} \tag{4}$$

Furthermore, the ratio of silica/alumina (*S/A*), iron/calcium (*I/C*), slagging index (R_s) and slag viscosity (S_R) was determined using Eqs. (5–8).

$$S/A = \frac{SiO_2}{Al_2O_3} \tag{5}$$

$$I/C = \frac{Fe_2O_3}{CaO} \tag{6}$$

$$R_s = R_{b/a} \times S \tag{7}$$

Table 4 Chemical composition of the various types of coal before and after conbustion

Trade name of coal	Before combustion													
	Al	Si	S	Cl	K	Ca	Ti	Mn	Fe	Zn	Rb	Sr	Cd	Zr
Ghazal BBQ	4.1	11			14.5	39	1	3.7	25	0.7	0.3	0.7		
Rehlat Saied	6	18	3.9		2.8	25	2.2	1	40			1.1		
Fire top	5.8	22			20	32	0.8	2	16	0.7	0.7			
Orinex				0.75	12.9	72	0.2	0.6	8.25			5.1		0.2
King Sford	5	24			20	38	0.7	1.2	10	0.5	0.4	0.1		0.1
Barbecue charcoal		8			25	42	1.5	4	17	0.6	0.5	1		0.4
Toppy	1.8	5.7			4	69	2.1	1.9	14			1.5		
Super Kima	5.6	33			16	24.9	0.9	1.6	17	0.5	0.3	0.2		
Burnable charcoal						4.5			18	0.5	1	68	8	
Volcano	1.2	9.7	0.4		5	70.6	1.1	0.4	11	0.1		0.4		0.1
Earthquake		4.1		21	9.8	60.4	0.2	0.7	3.2	0.2	0.1	0.3		
Royal BBQ		5.9			3	62.3	1.2	2.2	24		0.3	1.1		
Al Nakhla coal	2	6.6			2.5	62	1.6	1.2	22.5	0.3		1.2		0.1
Charcoal		5			8	76			9.7			1.3		
Al-Hijaz	5.5	21			9	36.7	1	1.6	24	0.6	0.4	0.2		
Medina		6	2.5		4.8	69.8	1	0.5	12			3.4		
Gwyn						15			3.4			81.6		
Bamboo charcoal					15	88.7	0.6					3.7		

Trade name of coal	After combustion														
	MgO	Al_2O_3	SiO_2	SO_2	Cl	K_2O	CaO	TiO_2	MnO	Fe_2O_3	ZnO	Rb_2O	SrO	ZrO_2	PbO
Ghazal BBQ	4	5	26	1.00		13.7	36	1	1.5	11	0.3	0.2	0.3		
Rehlat Saied		1	32	5.20		2.5	29.7	2	0.8	26	0.08	0.02	0.7		
Fire top			6	1.00		17	68	0.7	0.4	5.5	0.3	0.1	1		
Orinex		1	4	1.00	0.80	12.8	77		0.1	2.3	0.1		0.9		
King Sford						16	1		1	10	3.1	32.4	15	19	2.5
Barbecue charcoal		3.7	15.7			24	43.8	1	1.8	9	0.1	0.1	0.6	0.2	
Toppy		6.8	17	3.00		4	58.5	1.9	0.8	7.5	0.5				
Super Kima		11	51			12.6	15.2	0.6	0.7	8.2	0.2	0.2	0.1	0.1	0.1
Burnable charcoal		6.9	25.9	8.00		2.8	39	1.8	0.4	13.8	0.1		1.2	0.1	
Volcano						5.8	50.7	1.4	1.7	20.8	1	1.4	9.1	4.4	3.7
Earthquake			7.7	0.40	16.60	9	60.95	0.4	0.7	3.5	0.2	0.2	0.3	0.05	
Royal BBQ		3	20.47	5.30		4	60.6	0.5	0.1	5.6	0.03		0.4		
Al Nakhla coal	3.9	5.9	14.6	2.00		11.4	48.6	1	0.8	11.1	0.2	0.1	0.4		
Charcoal			13.9	0.80		7.8	54.7		0.5	18	0.5	0.2	3.3	0.1	
Al-Hijaz			9.9			8	50.9	1.3	0.8	27	0.5	0.5	0.9	0.2	
Medina		3.4	20.8	9.10		3.4	57.3	0.6	0.1	5			0.3		
Gwyn		4.4	13			8.8	53.3	0.9	0.7	16	0.4	0.2	2.3		
Bamboo charcoal			4.5			7	77.3			3.3			7.9		

$$S_R = \frac{SiO_2}{SiO_2 + Fe_2O_3 + CaO + MgO} \quad (8)$$

As shown in Table 6 (Electronic Supplementary Material), it is generally expected that slag deposition ($R_{b/a}$) will be achieved. Figure 2 shows that most CCRs (ash samples) contain more than 50% CaO and less than 30% SiO_2 with more than 15% K_2O. The ternary diagram in Fig. 3 classified most CCR samples as low acidity and indicates type C, which has a high calcium oxide ratio and is anticipated to have high melting temperatures and small deposits due to high concentration of Ca [16]. S and K types describe Super Kima and King Sford, respectively, which have a high risk of

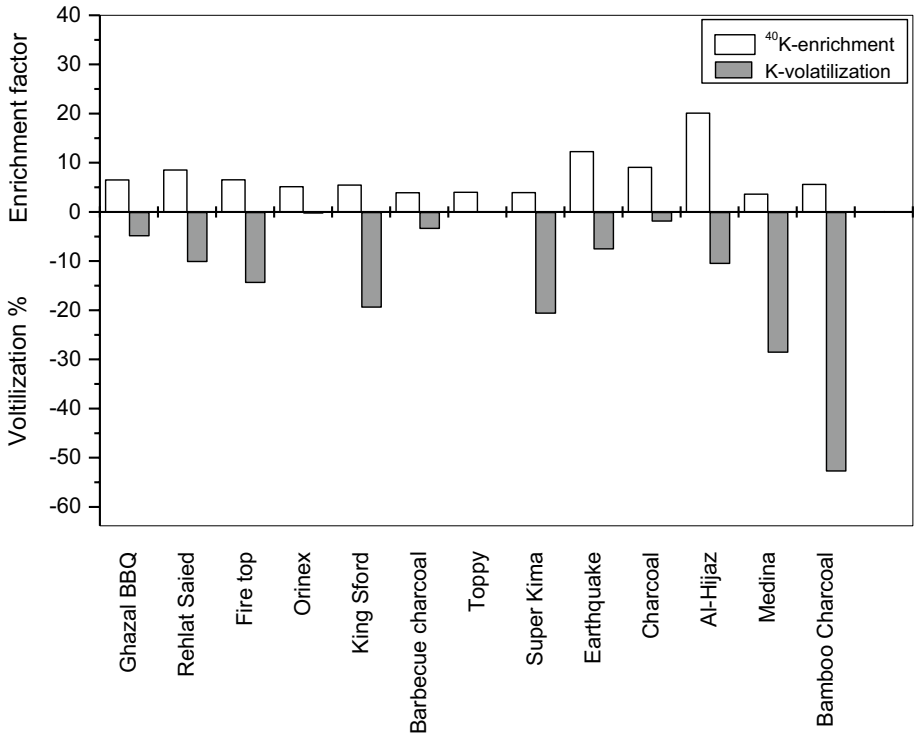

Fig. 1 Influence of burning of different types of coal on the volatilization rate (%) of K and enrichment factor of ^{40}K

Table 5 Determination of the K proportion (%) and 40 K radioactive (Bq kg^{-1}) in the various types of coal before and after combustion to estimate the 40 K activity per % K (Bq $\%K^{-1}$)

Trade name of coal	BC			AC		
	K (%)	^{40}K (Bq kg^{-1})	The radioactivity of ^{40}K per 1% K (Bq 1% K^{-1})	K (%)	^{40}K (Bq kg^{-1})	The radioactivity of ^{40}K per 1% K (Bq 1% K^{-1})
Ghazal BBQ	14.5	174	12.00	13.7	1130	82.48
Rehlat Saied	2.8	51	18.21	2.5	435	174.00
Fire top	20	300.4	15.02	17	1958	115.18
Orinex	12.9	251	19.46	12.8	1288	100.63
King Sford	20	347.8	17.39	16	1900	118.75
Barbecue charcoal	25	553	22.12	24	2150	89.58
Toppy	4	51.9	12.98	4	207	51.75
Super Kima	16	268	16.75	12.6	1050	83.33
Burnable charcoal		168		2.8	320	114.29
Volcano	5	68	13.60	5.8		
Earthquake	9.8	109	11.12	9	1337	148.56
Royal BBQ	3	38	12.67	4		
Al Nakhla coal	2.5	40	16.00	11.4		
Charcoal	8	100.6	12.58	7.8	913	117.05
Al-Hijaz	9	99	11.00	8	1990	248.75
Medina	4.8	76.7	15.98	3.4	277	81.47
Gwyn		49		8.8	462	52.50
Bamboo charcoal	15	238	15.87	7	1330	190.00

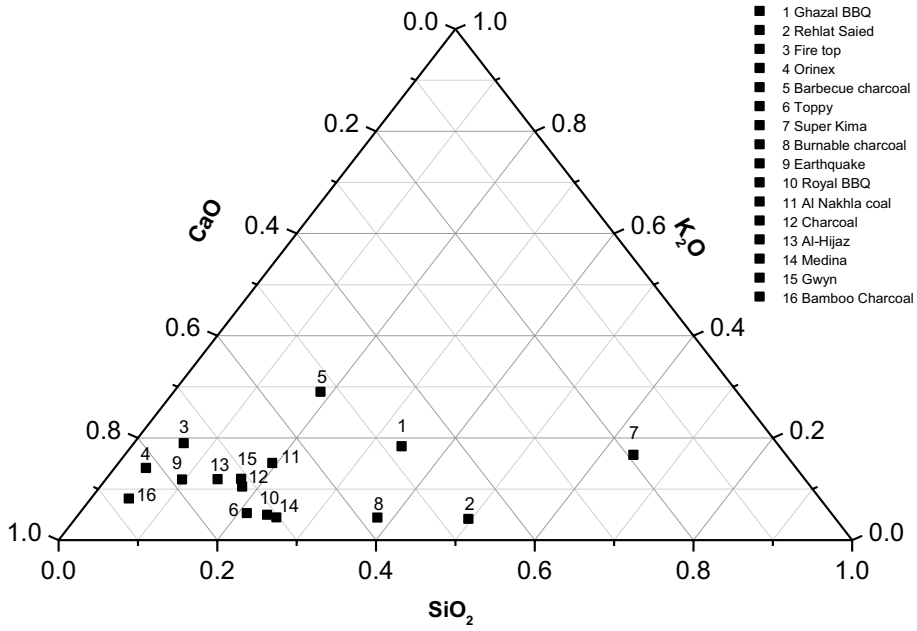

Fig. 2 SiO_2–CaO–K_2O ternary diagram after combustion process

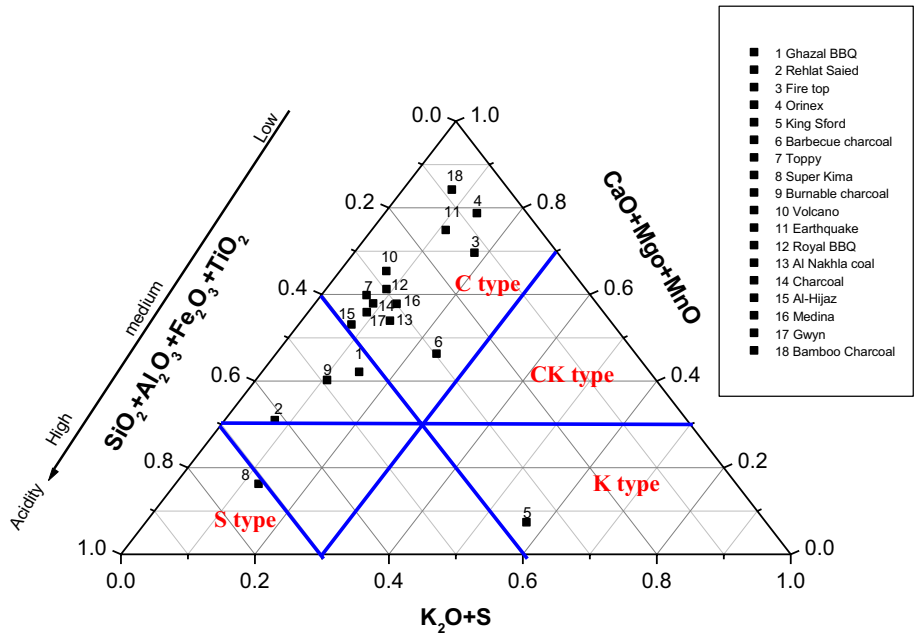

Fig. 3 $SiO_2 + CaO + K_2O + S + MgO + MnO + Al_2O_3 + Fe_2O_3 + TiO_2$ (AC) ternary diagram

deposition owing to the formation of silicates and presence of potassium [16].

Conclusion

The radioactivity of total Ra and ^{40}K in CCRs is 6–12 times higher than in the feed coal due to the removal of 10–15% carbon. Before burning, most coal samples have the ratios of $^{226}Ra/^{228}Ra$ close to the soil ratio (1.2). Radionuclides were measured in CCR samples to study the redistribution of these radionuclides and found that the majority of the samples had a concentration of ^{226}Ra less than ^{228}Ra, resulting the ratios of $^{228}Ra/^{226}Ra$ are relatively higher in CCRs than feed coal except for a small number of these samples. The effective annual dose rates were calculated and found to be 370.3 and 1797.5 μSv $year^{-1}$ for coal before and after burning, respectively. XRF was used to determine the proportions of Al, Si, K, Ca, Mn, Fe, Sr and Rb coal composition with variable concentrations obtained before and after the combustion process. The average concentration of ^{40}K (120 Bq kg^{-1} per 1% K_2O in CCRs) concentration

was calculated and its lower value was observed by half as compared to the literature value. Most CCR samples are low acidity and represent type C, which has a high calcium oxide ratio and is anticipated to have a high melting temperature and low deposits owing to high concentrations of Ca.

Acknowledgements This research was funded by Deanship of Scientific Research, Princess Nourah bent Adulrahman University through the Fast-track Research Funding Program. The authors would also like to thank editor-in-chief of Journal of Radioanalytical and Nuclear Chemistry and referees for their valuable comments and cooperation.

References

1. Trevisi R, Risica S, D'Alessandro M, Paradiso D, Nuccetelli C (2012) Natural radioactivity in building materials in the European Union: a database and an estimate of radiological significance. J Environ Radioact 105:11–20
2. Tadmor J (1986) Radioactivity from coal-fired power plants: a review. J Environ Radioact 4(3):177–204
3. Eisenbud M, Petrow HG (1964) Radioactivity in the atmospheric effluents of power plants that use fossil fuels. Science 144(3616):288–289
4. Coles DG, Ragaini RC, Ondov JM (1978) Behavior of natural radionuclides in western coal-fired power plants. Environ Sci Technol 12(4):442–446
5. Völgyesi P, Kis Z, Zs Szabó, Cs Szabó (2014) Using the 186-keV peak for ^{226}Ra activity concentration determination in Hungarian coal-slag samples by gamma-ray spectroscopy. J Radioanal Nucl Chem Lett 302:375–383
6. Beck HL, Gogolak C, Miller K, Lowder WM (1980) Perturbations on the natural radiation environment due to the utilization of coal as an energy source. U.S. Department of Energy, Washington
7. Zielinski RA, Budahn JR (1998) Radionuclides in fly ash and bottom ash: improved characterization based on radiography and low energy gamma-ray spectrometry. Fuel 77(4):259–267
8. Fardy J, McOrist G, Farrar Y (1989) Neutron activation analysis and radioactivity measurements of Australian coals and fly ashes. J Radioanal Nucl Chem Lett 133(2):217–226
9. Bem H, Wieczorkowski P, Budzanowski M (2002) Evaluation of technologically enhanced natural radiation near the coal-fired power plants in the lodz region of Poland. J Environ Radioact 61(2):191–201
10. Sanjuán MA, Argiz C (2012) The new European standard on common cements specifications EN 197-1:2011. Mater Constr 62:425–430
11. Argiz C, Menéndez E, Moragues A, Sanjuan MA (2015) Fly ash characteristics of Spanish coal-fired power plants. Afinidad 572:269–277
12. Council Directive 2013/59/Euratom of 5 Dec. (2013) Laying down basic safety standards for protection against the dangers arising from exposure to ionising radiation and repealing directives 89/618/Euratom. 90/641/Euratom. 96/29/Euratom. 97/43/Euratom and 2003/122/Euratom. L13, vol 57. ISSN: 1977-0677
13. Schroeyers W, Puertas F, Alonso M, Torres Carrasco M, Rivilla P, Gasco C, Trinidad JA, Suarez JA, Navarro N, Yague L, Mora JC, Orellana JG, Masque P, Hierro A, Bolıvar JP, Vazquez M, Quintana B (2015) In: Verdu´ G (ed) Introduction of the COST Action: COST TU1301 ''NORM4-building''. 48 Joint Congress 20 SEFM/15 SEPR (Spanish Society for Radiological Protection. Ed.) Valencia. Spain
14. Puertas F, García-Díaz I, Palacios M, Gazulla MF, Gómez MP, Orduña M (2010) Clinkers and cements obtained from raw mix containing ceramic waste as a prime material. Characterization, hydration and leaching studies. Cem Concr Compos 32:175–186
15. Sanjuan MA, Quintana B, Argiz C (2019) Coal bottom ash natural radioactivity in building materials. J Radioanal Nucl Chem Lett 319:91–99
16. García R, Pizarro C, Álvarez A, Lavín AG, Bueno JL (2015) Study of biomass combustion wastes. Fuel 148:152–159
17. Carlson CL, Adriano DC (1993) Environmental impacts of coal combustion residues. J Environ Qual 22:227–247
18. Ural S (2005) Comparison of fly ash properties from Afsin-Elbistan coal basin, Turkey. J Hazard Mater B119:85–92
19. Bundesanstalt für Geowissenschaften und Rohstoffe – Federal Institute for Geosciences and Natural Resources (BGR) (2009) Reserves, resources and availability of energy resources—annual report 2009, BGR, Hannover, Germany. www.bgr.bund.de
20. Puertas F, Alonso MM, Torres-Carrasco M, Rivilla P, Gasco C, Yagüe L, Suárez JA, Navarro N (2015) Radiological characterization of anhydrous/hydrated cements and geopolymers. Constr Build Mater 101:1105–1112
21. Lauer NC, Hower JC, Hsu-Kim H, Taggart RK, Vengosh A (2015) Naturally occurring radioactive materials in coals and coal combustion residuals in the United States. Environ Sci Technol 49(18):11227
22. Pandit GG, Sahu SK, Puranik VD (2011) Natural radionuclides from coal fired thermal power plants—estimation of atmospheric release and inhalation risk. Radioprotection 46(6):S173–S179
23. Swanson VE (1976) Collection, chemical analysis, and evaluation of coal samples in 1975. U.S. Department of the Interior, Geological Survey, Washington
24. Allam KhA, Ahmed Z, El-Sharkawy S, Salman A (2017) Analysis and statistical treatment of 238U series isotopic ratios using gamma-ray spectrometry in phosphate samples Radiat. Prot Environ 40(3&4):110
25. European Commission (1999) Radiation protection 122-radiological protection principles concerning the natural radioactivity of building materials. Directorate General Environment. Nuclear Safety and Civil Protection. https://ec.europa.eu/energy/sites/ener/files/documents/112.pdf. Accessed 27 Jul 2018
26. Markkanen M (1995) Radiation dose assessments for materials with elevated natural radioactivity. Report STUK-B-STO 32. Radiation and Nuclear Safety Authority-STUK. Helsinki. Iceland
27. Stojanovska Z, Nedelkovski D, Ristova M (2010) Natural radioactivity and human exposure by raw materials and end product from cement industry used as building materials. Radiat Meas 45:969–972
28. UNSCEAR (1998) Sources, effects and risk of ionizing radiation. United Nations, New York
29. UNSCEAR (1993) Exposure from natural sources of radiation. United Nations, New York
30. Yang Y (2005) Radioactivity concentrations in soils of the Xiazhuang granite area, China. Appl Radiat Isot 63:255–259
31. Mohanty AK, Sengupta D, Das SK, Saha SK (2004) Natural radioactivity and radiation exposure in the high background area at Chatrapur beach placer deposit of Orissa, India. J Environ Radioact 75:15–33
32. Xiao R, Chen X, Wang F, Yu G (2011) The physicochemical properties of different biomass ashes at different ashing temperature. Renew Energy 36:244–249
33. Bridgeman TG, Darvell LI, Jones JM, Williams PT, Fahmi R, Bridgewater AV et al (2007) Influence of particle size on the analytical and chemical properties of two energy crops. Fuel 86:60–72

34. Fryda L, Sobrino C, Glazer M, Bertrand C, Cieplik M (2012) Study of ash deposition during coal combustion under oxyfuel conditions. Fuel 92:308
35. Vamvuka D, Pitharoulis M, Alevizos G, Repouskou E, Pentari D (2009) Effects during combustion of lignite/biomass blends in fluidized bed. Renew Energy 34:2662

Publisher's Note Springer Nature remains neutral with regard to jurisdictional claims in published maps and institutional affiliations.